

微波電漿化學氣相沉積法合成準直性碳奈米管及碳奈米尖錐之 奈米製程與場發射性質

研究生:林奕同

指導教授: 郭正次 教授

國立交通大學材料科學與工程研究所

摘要

近年來以碳基奈米結構材料所製成的場發射元件上獲得舉世的注目。特別是碳奈米管(CNTs)及碳奈米尖錐(CNCs)，由於它們具備高的深寬比形貌以及奈米級的發射極半徑。影響碳奈米結構場發射性質的因素包括其結構尺寸大小、排列方向、表面形貌、碳的鍵結、管束成長密度和與基材的附著性..等等，而這些因素都與製程參數有關，因此如何利用製程參數來操控奈米結構是眾多重要的課題之一。本研究以微波電漿化學氣相沉積(MPCVD)法合成具準直性碳奈米管與碳奈米尖錐在矽基材上，使用10 nm的鈷膜當作觸媒， H_2 、 NH_3 、Ar、 C_2H_2 和 CH_4 當作氣體原料。在每一階段製程的奈米結構與性質利用掃描式電子顯微鏡(SEM)、穿透式電子顯微鏡(TEM)、電子繞射(ED)、拉曼光譜儀(Raman spectroscopy)、歐傑電子能譜儀(AES) 和 以I-V 量測儀進行分析。

氫電漿前處理結果顯示高的基材溫度相依於大的氣氛的壓力及微波功率，在條件為9 Torr 的氫氣壓力及400 W 的微波功率之氫電漿前處理下，有適當的觸媒平均粒徑和數目密度。在不同的氣體源與外加負偏壓

所成長出的碳管具準直性，可能是由於電漿自我偏壓、負偏壓增強電漿鞘能量或是較高的管束密度所造成的。對於成長時間影響碳管的準直性結果顯示，成長時間太長會因為不同觸媒毒化速率的不同而造成捲曲狀碳管的形成。在場發射性質方面以無偏壓輔助成長 10 分鐘的準直碳管表現最佳，其開啟電場 (E_{to}) $\sim 4.4 \text{ V}/\mu\text{m}$ ；起始電場 (E_{th}) $\sim 8.26 \text{ V}/\mu\text{m}$ ；場發射增強因子 $\beta \sim 4096$ ，而在 $10 \text{ V}/\mu\text{m}$ 的電場下可達 $88.7 \text{ mA}/\text{cm}^2$ 。但經過多次循環的場發射量測後碳管會從矽基材剝落，推測原因為碳管與基材附著性不佳所以無法承受電場的破壞。根據不同施加負偏壓及 H_2/CH_4 比例影響下成長碳奈米尖錐結果顯示，碳奈米尖錐的合成必須在偏壓大於 -150 V 且 H_2/CH_4 需小於 $80/5$ (sccm/sccm)。準直碳奈米尖錐合成溫度皆低於 650°C 。尖錐的高度隨著負偏壓和 H_2/CH_4 比例上升而增高。相對的，尖錐的底部寬度及頂端角度隨著負偏壓和 H_2/CH_4 比例的上升而減小。從 SEM 結果推測碳奈米尖錐的形貌可能是在電漿環境中碳沉積與離子蝕刻互相競爭所產生的結果。拉曼光譜、AES、TEM 及 ED 分析顯示其為一個多晶石墨層、非晶質矽和非晶質碳混合物的尖錐，且在尖錐頂部及底部都有鈷觸媒的存在。在場發射性質上碳奈米尖錐展現出較碳管優異的性質，其開啟電場 (E_{to}) $\sim 5.0 \text{ V}/\mu\text{m}$ ；起始電場 (E_{th}) $\sim 6.99 \text{ V}/\mu\text{m}$ ；場發射增強因子 $\beta \sim 4993$ ，而在 $10 \text{ V}/\mu\text{m}$ 的電場下更可達 $173.42 \text{ mA}/\text{cm}^2$ 。碳奈米尖錐可以承受高電場長時間的場發射量測而且有穩定的發射電流，顯示出碳奈米尖錐對基材的附著性比碳奈米管優異。

Nanofabrication and field emission properties of the well-aligned carbon nanotubes and carbon nanocones synthesized by MPCVD

Graduate Student: Yi-Tung Lin

Advisor: Cheng-Tzu Kuo

**Institute of Materials Science and Engineering
National Chiao Tung University**

Abstract

Applications of the carbon nanostructured materials to fabricate the field emission (FE) devices are gained greater attention in recent years in the world, especially, the carbon nanotubes (CNTs) and the carbon nanocones (CNCs) due to their high aspect ratios morphologies and nanoscale field emitter radius. There are many factors governing the FE properties of carbon nanostructures, such as size, orientation, morphologies, bonding structure, tube number density and adhesion with the substrate, depending on the process parameters. Therefore, way to manipulate the nanostructures is one of the important topics. In this study, processes were developed to synthesize the well-aligned CNTs and CNCs on Si substrate by microwave plasma chemical vapor deposition (MPCVD), using 10 nm Co film as a catalyst and H₂, NH₃, Ar, C₂H₂ and CH₄ as source gases. The carbon nanostructure and properties at each processing step were characterized by scanning electron microscopy (SEM), transmission electron microscopy (TEM), electron diffraction (ED), Raman spectroscopy, Auger electron spectroscopy (AES), and I-V measurements.

On the pretreatment process, the results indicate the greater substrate temperature are depending on the greater gas pressure and microwave power. Under 9 Torr H₂ pressure and 400 W microwave power plasma pretreatment condition shows appropriate number density and small average catalyst particle sizes. The CNTs show the aligned orientation which are synthesized by different gas sources and applied negative bias, it may be due to plasma self-bias potential, applied negative bias enhance plasma sheath

potential or greater tube number density induced. The result of CNTs synthesized under different growth time reveals wave-like CNTs easily produced on long time growth, it may be induced by each CNT having different catalyst poisoned rate. The well-aligned CNTs which were grown under 10 min without applied bias shows the best FE properties, It's $E_{to} \sim 4.4 \text{ V}/\mu\text{m}$, $E_{th} \sim 8.26 \text{ V}/\mu\text{m}$, field enhancement factor $\beta \sim 4096$, and $J \sim 88.7 \text{ mA}/\text{cm}^2$ at $10 \text{ V}/\mu\text{m}$. However, the CNTs after several cycles of I-V measurement will striped from the substrate. It may be due to the bad adhesion between the CNTs and substrate.

The results of different applied negative bias and H_2/CH_4 ratio on CNCs growth show the well-aligned CNCs preferred to synthesize under above -150 V bias and lower H_2/CH_4 ratio ($< 80/5 \text{ sccm}/\text{sccm}$). It is significant to note that the growth temperature of well-aligned CNCs is below 650°C . The Height of CNCs will increase with an increase of applied negative bias and H_2/CH_4 ratio. In contrary, the bottom diameter and apex angle of CNCs decrease with a decrease of applied negative bias and H_2/CH_4 ratio. The morphology of CNCs may be produced by the competition between the carbon deposition and ion etching under plasma bulk. The results of Raman spectrum, AES, TEM, and ED analysis indicated the CNC is the cone-shaped mixture of polycrystalline graphite, amorphous Si and amorphous carbon, where the existence of Co catalysts are both in the tip and bottom of the CNC. The CNCs exhibit better FE properties than CNTs, its $E_{to} \sim 5.0 \text{ V}/\mu\text{m}$, $E_{th} \sim 6.99 \text{ V}/\mu\text{m}$, field enhancement factor $\beta \sim 4993$, and $\sim 173.42 \text{ mA}/\text{cm}^2$ at $10 \text{ V}/\mu\text{m}$. The CNCs can bear long time measurement under high electric field and with stable emission current. It indicates that the CNCs have the better adhesion with the substrate than CNTs.

Contents

| | |
|---|-------|
| Chinese abstract..... | I |
| English abstract..... | III |
| Contents..... | V |
| List of symbols..... | IX |
| Table captions..... | X I |
| Figure captions..... | X III |
| Chapter 1 Introduction..... | 1 |
| 1-1 Introduction to carbon nanotubes (CNTs)..... | 1 |
| 1-2 Introduction to carbon nanocones (CNCs)..... | 4 |
| 1-3 Motivation of this research..... | 6 |
| Chapter 2 Literature reviews..... | 7 |
| 2-1 Structures, properties, and nanofabrications of CNTs..... | 7 |
| 2-1-1 Structures and properties of CNTs..... | 7 |
| 2-1-2 Nanofabrications of CNTs..... | 13 |
| 2-2 Applications of CNTs..... | 19 |
| 2-2-1 Hydrogen storage..... | 19 |
| 2-2-2 Lithium intercalation..... | 19 |
| 2-2-3 Electrochemical super capacitors..... | 20 |
| 2-2-4 Field emitting devices..... | 20 |
| 2-2-5 Transistors..... | 21 |
| 2-2-6 Nanoprobes and sensors..... | 21 |
| 2-2-7 Composite materials..... | 22 |

| | |
|---|-----------|
| 2-3 Structure, properties and nanofabrication of CNCs..... | 25 |
| 2-4 Theory of field emission..... | 30 |
| 2-5 Overview of field emission devices..... | 33 |
| Chapter 3 Experimental methods..... | 39 |
| 3-1 Flow chart and process descriptions..... | 39 |
| 3-2 Raw materials..... | 40 |
| 3-3 Microwave plasma chemical vapor deposition system..... | 41 |
| 3-4 Procedure of carbon nanostructures deposition..... | 42 |
| 3-5 Analysis methods..... | 43 |
| 3-5-1 Scanning electron microscopy (SEM)..... | 43 |
| 3-5-2 Transmission electron microscopy (TEM) and sample preparation.... | 43 |
| 3-5-3 Raman spectorscopy..... | 43 |
| 3-5-4 Auger electron spectroscopy (AES) | 44 |
| 3-5-5 Field Emission Measurement..... | 44 |
| Chapter 4 Results and discussion..... | 52 |
| 4-1 Effects of H plasma pretreatment on catalyst particle formation..... | 52 |
| 4-2 Effects of bias, forest supporting and deposition time on CNTs growth.... | 53 |
| 4-3 Raman spectra of CNTs..... | 55 |
| 4-4 Field emission properties of the aligned CNTs..... | 56 |
| 4-5 Effect of post plasma trimming on structure and properties of CNTs..... | 58 |
| 4-6 TEM and HRTEM of CNTs..... | 60 |
| 4-7 Effects of applied bias and H ₂ /CH ₄ ratio on CNCs growth..... | 61 |
| 4-8 Raman and AES spectra of CNCs..... | 63 |
| 4-9 Field emission properties of CNCs..... | 64 |

Chapter 5 Conclusions.....96
Chapter 6 Prospective.....98
References.....99



List of symbols

| | |
|----------|--|
| a_1 | Vector of graphene sheet |
| a_2 | Vector of graphene sheet |
| a-C | Amorphous Carbon |
| AES | Auger Electron Spectroscopy |
| AFM | Atomic Force Microscope |
| APC | Auto Pressure Controller |
| C_{60} | Buckminsterfullerene |
| C_h | Chiral Vector |
| CNTs | Carbon Nanotubes |
| CNCs | Carbon Nanocones |
| CRT | Cathode-Ray Tube |
| CVD | Chemical Vapor Deposition |
| DC | Direct Current |
| DLC | Diamond-Like Carbon |
| e | Charge of the electron |
| E | Electric Field |
| ECRCVD | Electron Cyclotron Resonance CVD |
| ED | Electron Diffraction |
| ELD | Electro Luminescent Display |
| E_{th} | Threshold Electric Field |
| E_{to} | Turn on Electric Field |
| FCC | Face Center Cubic |
| FE | Field Emission |
| FED | Field Emission Display |
| FET | Field Effect Transistor |
| F-N | Fowler-Nordheim |
| h | Planck constant |
| HOPG | Highly Oriented Pyrolytic Graphite |
| HRSEM | High Resolution Scanning Electron Microscopy |
| HRTEM | High Resolution Transmission Electron Microscopy |
| I | Field emission current |
| IC | Integrated Circuit |
| J | Current density |

| | |
|-----------|--|
| LCD | Liquid Crystal Display |
| k | Boltzmann's constant |
| m_e | The mass of the electron |
| m_i | The mass of the ion |
| MPCVD | Microwave Plasma CVD |
| MP-HF-CVD | Microwave Plasma-Hot Filament-CVD |
| MWNTs | Multi-Walled Carbon Nanotubes |
| OLED | Organic Light Emitting Display |
| PECVD | Plasma Enhance CVD |
| PE-HF-CVD | Plasma Enhance-Hot Filament-CVD |
| PDP | Plasma Display Panel |
| PVD | Physical Vapor Deposition |
| r | Tip radius of the emitter tip |
| RF | Radio Frequency |
| SEM | Scanning Electron Microscopy |
| STM | Scanning Tunneling Microcopy |
| SWNTs | Single-Walled Carbon Nanotubes |
| T | Time |
| T_e | The electron temperature |
| TEM | Transmission Electron Microscopy |
| V | Applied Voltage |
| V' | Self-bias potential |
| VFD | Vacuum Fluorescent Display |
| VME | Vacuum Micro Electronics |
| W_0 | The energy difference between an electron at rest outside and inside of the metal. |
| W_f | The energy difference between the Fermi level and the bottom of the conduction band. |
| α | Effective emission area |
| β | Field enhancement factor |
| β' | Geometric correction factor |
| θ | Chiral angle |
| θ' | The angle of the cone |
| ϕ | Work Function |

Table captions

| | | |
|------------------|--|----|
| <u>Table 1-1</u> | Carbon nanotube-A time line ^[http://www.pa.msu.edu] | 3 |
| <u>Table 2-1</u> | The threshold electrical field for different materials at 10 mA/cm ² current density ^[Zhu-98-1471] | 11 |
| <u>Table 2-2</u> | The properties of graphite, diamond, C ₆₀ and carbon nanotube ^[http://www.pa.msu.edu] | 11 |
| <u>Table 2-3</u> | Summaries of the synthetic methods of CNCs in the literatures..... | 27 |
| <u>Table 2-4</u> | Characteristics of solid state and VME device ^[Zhu-2001-7] | 36 |
| <u>Table 2-5</u> | Comparison of FED with other Flat Panel Displays ^[Zhu-2001-290] | 38 |
| <u>Table 3-1</u> | Process conditions of hydrogen plasma pretreatment for Co-coated Si substrate | 48 |
| <u>Table 3-2</u> | Specimen designation of the as-grown CNTs on silicon wafer and their process conditions..... | 49 |
| <u>Table 3-3</u> | Process conditions of plasma post-treatment for CNTs of Specimen A5..... | 50 |
| <u>Table 3-4</u> | Specimen designation of as-grown CNCs on silicon wafer and their process conditions. | 51 |
| <u>Table 4-1</u> | I _G /I _D ratios of as-growth CNTs under different applied bias..... | 74 |
| <u>Table 4-2</u> | FE properties of different negative bias applied on CNTs growth..... | 75 |
| <u>Table 4-3</u> | The field enhancement factor β of different negative applied bias on CNTs growth..... | 76 |
| <u>Table 4-4</u> | FE properties of CNTs grown on different growth time..... | 77 |

Table 4-5 I_G/I_D ratios of as-grown and H-plasma and N-plasma post treated CNTs.....81

Table 4-6 I_G/I_D ratios of as-grown and Ar-plasma and ammonia-plasma post treated CNTs
.....82

Table 4-7 FE properties of post plasma treated CNTs.....83

Table 4-8 FE properties of as-grown CNCs onder different negative applied bias.....94

Table 4-9 The field enhancement factor β of as-grown CNCs (Specimen B5).....95



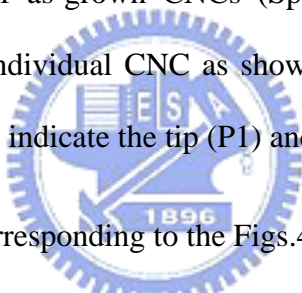
Figure caption

| | | |
|------------------|---|----|
| <u>Fig. 1-1</u> | Schematic diagram of C ₆₀ structure..... | 2 |
| <u>Figs. 1-2</u> | HRTEM images of carbon nanotubes with increasing numbers of concentric tubes-one to five layers seen in (a) to (e), respectively ^[Ebbesen-97-115] | 2 |
| <u>Figs. 1-3</u> | (a) and (b) are SEM images of CNCs (c) HRTEM images of CNC ^[Zhang-03-472] ... | 5 |
| <u>Figs. 1-4</u> | HRTEM images and Fourier filtering transformation (FFT) of amorphous CNC (a) the end section and (b) lateral section of an individual CNC ,where show the nanocrystalline graphite embedded in lateral section of CNC ^[Tasi-02-1281] | 5 |
| <u>Fig. 2-1</u> | Spatial vector representation on 2D graphene sheet ^[Dresselhaus-96-756] | 8 |
| <u>Fig. 2-2</u> | CNT structures of armchair, chiral and zigzag tubules. ^[Dresselhaus-96-756] | 8 |
| <u>Fig. 2-3</u> | The 2D graphene sheet is shown different electrical conductivity of zigzag, armchair and chiral nanotubes depending on its chirality. ^[Saito-92-2204] | 9 |
| <u>Fig. 2-4</u> | schematic drawing of arc-discharge system ^[Ebbesen-92-220] | 14 |
| <u>Fig. 2-5</u> | schematic drawings of a laser ablation apparatus ^[Guo-95-243] | 15 |
| <u>Fig. 2-6</u> | schematic drawings of thermal CVD system ^[Lee-2000-3397] | 16 |
| <u>Fig. 2-7</u> | schematic drawing of MPCVD apparatus ^[Qin-98-3437] | 17 |
| <u>Fig. 2-8</u> | schematic drawing of PE-HF-CVD apparatus ^[Kurt- 00-1723] | 18 |
| <u>Fig. 2-9</u> | schematic drawing of MPCVD apparatus ^[Tsai-01-NCTU] | 18 |
| <u>Fig. 2-10</u> | Emitting image of fully sealed CNT-field emission display at color mode with red, green and blue phosphor columns ^[Choi-99-3129] | 22 |

| | | |
|-------------------|--|----|
| <u>Fig. 2-11</u> | Schematic cross section of the FET devices. A single SWNT or MWNT is bridges the gap between two gold electrodes. The Si substrate which is covered by a layer of SiO ₂ , acts as a back-gate ^[Martel-98-2447] | 23 |
| <u>Fig. 2-12</u> | Schematic drawing of the spin-resolved CNT-STM. A CNT is acting tunneling tip in proximity to a magnetic sample with spin polarization P _s . The long mean-free path in the CNT is used to transport the tunnel current to two oppositely magnetized ferromagnetic electrodes. The spin polarization in the electrodes P _f causes an asymmetry between the currents through them (I ₁ and I ₂) ^[Orgass-01-281] | 23 |
| <u>Figs. 2-13</u> | (a) Tapping mode AFM image scanning by conventional Si tips (b) Tapping mode AFM image of CNTs tips scanning which provide better resolution than Si tips with the same specimen ^[Dai-96-147] | 24 |
| <u>Figs. 2-14</u> | Overview of the fabrication of CNT nanotweezers (A) schematic drawing the deposition of two independent metal electrodes and subsequent attachment of CNT and (B) SEM images are corresponding to the (A) , where the scale bar equal to 1 μm . The scale bar of inset HRSEM image is equal to 200 nm ^[Kim-99-2148] | 24 |
| <u>Fig. 2-15</u> | The possible tip structure with cone shape, in which the pentagons are included..... | 26 |
| <u>Figs. 2-16</u> | Energy diagrams of vacuum-metal boundary (a) without external electric field (b)with an external electric field ^[Tarntair-90-91] | 33 |
| <u>Fig. 2-17</u> | Perspective view of an FED in which one emitter array is shared by a red, green, and blue subpixel ^[Zhu-2001-293] | 37 |
| <u>Fig. 2-18</u> | The Spindt microfabricated field emitter arrays ^[Zhu-2001-106] | 37 |

| | | |
|------------------|--|----|
| <u>Fig. 3-1</u> | Flow Chart of the experiment..... | 45 |
| <u>Fig. 3-2</u> | Schematic drawing of MPCVD system..... | 46 |
| <u>Fig. 3-3</u> | Schematic drawing of MPCVD reactor..... | 47 |
| <u>Figs. 4-1</u> | Morphologies of catalyst film after hydrogen plasma pretreatment under conditions PT1 and PT2 at different magnification, respectively..... | 66 |
| <u>Figs. 4-2</u> | Morphologies of catalyst film after hydrogen plasma pretreatment under conditions PT3 and PT4 at different magnification, respectively..... | 67 |
| <u>Figs. 4-3</u> | Morphologies of catalyst film after hydrogen plasma pretreatment under conditions PT1 and PT5 at different magnification, respectively..... | 68 |
| <u>Figs. 4-4</u> | Morphologies of catalyst film after hydrogen plasma pretreatment under conditions PT6 and PT7 at different magnification, respectively..... | 69 |
| <u>Figs. 4-5</u> | Morphologies of as-grown CNTs under different precursor gases. Specimens A1, A2 and A3 are corresponding to the image (a), (b), and (c), respectively...70 | |
| <u>Figs. 4-6</u> | High magnification SEM image of (a) Specimen A2 (b) Specimen A3..... | 71 |
| <u>Figs. 4-7</u> | Morphologies of as-grown CNTs under different applied bias (a) 0 V (b) -50 V (c) -150 V (d) -250 V..... | 72 |
| <u>Figs. 4-8</u> | Morphologies of as-grown CNTs under different grown time (a) 5 min (b) 10 min (c) 15 min (d) 15 min..... | 73 |
| <u>Figs. 4-9</u> | Raman spectra of as-growth CNTs under different applied bias (a) 0 V (b) -50 V (c) -150 V (d) -250 V..... | 74 |
| <u>Fig. 4-10</u> | J-E curve of different negative applied bias on CNTs growth..... | 75 |

| | | |
|-------------------|--|----|
| <u>Figs. 4-11</u> | F-N plots of different negative substrate bias applied on CNTs growth (a) 0 V (b) -50 V (c)-150 V (d) -250 V..... | 76 |
| <u>Fig. 4-12</u> | J-E curves of different growth time of CNTs..... | 77 |
| <u>Figs. 4-13</u> | Morphologies of stripped CNTs after I-V measurement. The image (a) is corresponding to the image (b) in high magnification..... | 78 |
| <u>Figs. 4-14</u> | Morphologies of as-grown CNTs after H-plasma post treated (a) top view (b) inclined view | 79 |
| <u>Figs. 4-15</u> | Morphologies of as-grown CNTs after N-plasma post treated (a) top view (b) inclined view | 79 |
| <u>Figs. 4-16</u> | Morphologies of as-grown CNTs after Ar-plasma post treated (a) top view (b) inclined view | 80 |
| <u>Figs. 4-17</u> | Morphologies of as-grown CNTs after ammonia-plasma post treated (a) top view (b) inclined view | 80 |
| <u>Figs. 4-18</u> | Raman spectra of as-grown and H-plasma and N-plasma post treated CNTs | 81 |
| <u>Fig. 4-19</u> | Raman spectra of as-grown and Ar-plasma and ammonia-plasma post treated CNTs..... | 82 |
| <u>Figs. 4-20</u> | J-E curves of CNTs under different plasma post treated (a) H-plasma (b) N-plasma (c)Ar-plasma (d)ammonia-plasma..... | 83 |
| <u>Figs. 4-21</u> | (a) and (b) TEM images of as-grown CNTs (Specimen A5). It shows the CNTs have no catalyst encapsulated in the tip as indicate by white arrowhead. The bamboo structure is observed in the inner channel of CNTs..... | 84 |

| | | |
|-------------------|---|----|
| <u>Figs. 4-22</u> | (a), (b), and (c) are the corresponding HRTEM images which show the tip, stem and bottom of individual CNT, respectively..... | 85 |
| <u>Figs. 4-23</u> | Morphologies of as-grown CNCs under different negative applied bias. (a) 0 V (b) -50 V (c) -150 V (d) -200 V (e) -300 V..... | 86 |
| <u>Figs. 4-24</u> | (a) and (b) are the high magnification SEM images of Specimen B5. The image (b) is corresponding to the mage (a) at high magnification..... | 87 |
| <u>Figs. 4-25</u> | (a) to (d) show the morphologies of as-grown CNCs under different H ₂ /CH ₄ flow ratio..... | 88 |
| <u>Fig.4-26</u> | Raman spectrum of as-grown CNCs for Specimen B5..... | 89 |
| <u>Figs. 4-27</u> | (a) AES spectra of as-grown CNCs (Specimen B5), where P1 and P2 are detected point of individual CNC as shown in corresponding SEM image (b). The arrowheads are indicate the tip (P1) and bottom (P2) of individual CNC...  | 90 |
| <u>Figs. 4-28</u> | AES spectra are corresponding to the Figs.4-27 at selective segment..... (a) the AES spectrum of carbon (b) reference spectrum of carbon ^[Lin-01-126] (c) the AES spectrum of cobalt (d)reference spectrum of cobalt ^[Ferguson-98-63] | 91 |
| <u>Figs. 4-29</u> | (a) TEM bright field image of as-grown CNCs (specimen B5). ED pattern of (b), (c) and (d) are corresponding to image (a) in select area as indicate by arrowhead..... | 92 |
| <u>Figs. 4-30</u> | HRTEM images of as-grown CNCs (Specimen B5). image (a) and (b) show the tip of two individual CNCs..... | 93 |
| <u>Figs. 4-31</u> | J-E curves of as-grown CNCs under different applied bias (a) -50 V (b) -150 V (c) -200 V (d) -300 V..... | 94 |
| <u>Figs. 4-32</u> | F-N plot of as-grown CNCs (Specimen B5)..... | 95 |

Figs. 4-33 I-T curve of as-grown CNCs (Specimen B5).....95



